

Cosmic-Ray Nuclear Interactions in Gases*

W. W. BROWN†

Department of Physics, Duke University, Durham, North Carolina

(Received August 14, 1953)

The natural rates of occurrence, in the gases He, N, Ne, and A, of nuclear interactions of the cosmic ray *N* component in which more than 8 Mev are given to charged secondary particles, have been measured. The rates per gram atom of the four gases are in about the same ratio as their geometric nuclear cross sections. An integrated flux of *N* rays of $6.0 \times 10^{-3} \text{ cm}^{-2} \text{ sec}^{-1}$ would produce the observed rates of occurrence of nuclear interactions if the cross section were geometric. The rates in argon, measured at sea level and 10 600-ft elevation, correspond to an absorption mean free path in air of $132 \pm 4 \text{ g cm}^{-2}$ for the total flux of *N* rays. The interactions, 2783 in total, were observed in the gas of a cloud chamber filled to 5 atmos pressure. Inside the cloud chamber was placed a system of wires forming an ionization chamber. An expansion was initiated whenever a pulse from the ionization chamber corresponding to an energy release of more than 8 Mev (1.5 Po alpha) occurred. Fast reduction of the high voltage after electron collection was over permitted track formation on the positive ions. Of the nuclear interactions produced in argon about 20 percent are produced by charged particles at the higher elevation, and about 15 percent at sea level.

I. INTRODUCTION

THE present report is of an experiment in which the relative cross sections for nuclear interaction that the elements helium, nitrogen, neon, and argon present to the *N* component of cosmic rays are measured. The method employed is to count the number of cosmic-ray nuclear interactions occurring, over a measured time interval, in the gas of a cloud chamber successively filled with these atoms. The relative rates of occurrence of nuclear interactions in the gases may then be compared with the relative geometric cross sections of their nuclei. Rather than use random expansions, which would make the experiment prohibitively long, a detector, offering relatively little experimental bias, was placed inside the chamber to act as a triggering device. The details of the detecting system, experimental results, and corrections applied to them are described below.

II. EXPERIMENTAL ARRANGEMENT

The cloud chamber, of the expansion type with rubber diaphragm, was designed to operate at pressures

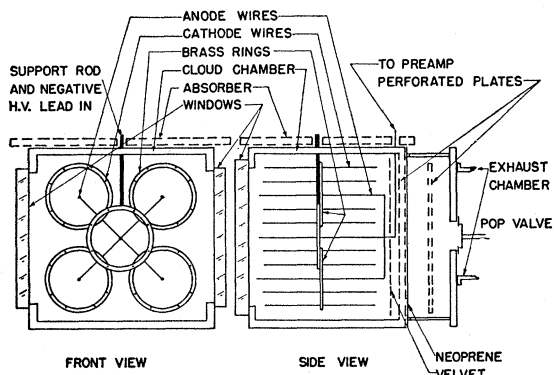


Fig. 1. Two perpendicular sections showing the location of the ionization chamber assembly inside the cloud chamber.

* Assisted by the joint program of the U. S. Office of Naval Research and the U. S. Atomic Energy Commission.

† Now at the University of California, Berkeley, California.

up to 75 lb in.⁻². It has a useful area, as viewed by the camera, of 10 in.×10 in. and an illuminated depth of 8 in.

Five ionization chambers are mounted inside the cloud chamber (Fig. 1). Each ionization chamber consists of eight parallel and equally spaced cathode wires $\frac{1}{8}$ -in. diameter×8-in. length held at their midpoints by a thin 4-in. diameter brass ring and all equidistant from and parallel to a similar central anode wire. The cathodes of the five chambers are tied together and the whole system supported by the high-voltage lead

TABLE I. Conditions of operation of the cloud chamber and the numbers of photographs, sensitive times, and numbers of nuclear interactions involving one or more charged particles observed under these conditions.

Atmospheric depth, g cm ⁻²	700	700	700	700	700	700	1032
Gas	A	A	A	Ne	N	He	A
Pressure, lb in. ⁻²	71	71	71	71	60	72	74
Temp. °C	19	19	19	21	18	20	17
Brass above chamber, in.	0	0.25	0.75	0	0	0	0
No. of photographs	2713	431	1026	104	2156	832	1948
Operating time, min	30 548	5017	11 665	1415	17 006	12 802	57 900
Dead time per picture, min	8.43	8.43	8.43	8.43	4.95	8.43	8.43
Sensitive time, min	7680	1382	3005	537	6345	5780	41 500
No. of nuclear interactions	1112	179	379	67	439	106	501

passing through the cloud chamber roof. The anodes, also in parallel, are connected to the amplifying system through another insulated lead passing through the cloud chamber roof.

The amplified pulse resulting from collection at the anode of the electrons produced by a charged particle traversing the sensitive volume serves to trigger the cloud-chamber expansion if it is larger than a prescribed size. It also initiates the reduction of the high negative voltage of the cathode (1 to 1.5 kilovolts) to zero or a slightly positive value by electronic means. The voltage reduction is rapid enough so that the positive ions along the path of the particle are not appreciably moved. The small displacement given to them is somewhat compensated when the cathode is allowed to

go positive during cutoff. Droplet formation on these ions thus permits observation of the track of a pulse producing particle.

Isoamyl alcohol was used as the cloud chamber vapor because it does not capture electrons easily and so does not interfere with the operation of the ionization chamber. With this vapor an expansion ratio of 1.15 is required for track formation in the monatomic gases and 1.25 in nitrogen.

The operational details of the cloud chamber and control system have been published elsewhere.¹

The high-voltage input lead was made tubular so that through it a polonium-alpha source on the end of a thin wire could be manually inserted into or retracted from the central ionization chamber. Pulses generated by this source were used to calibrate a discriminator

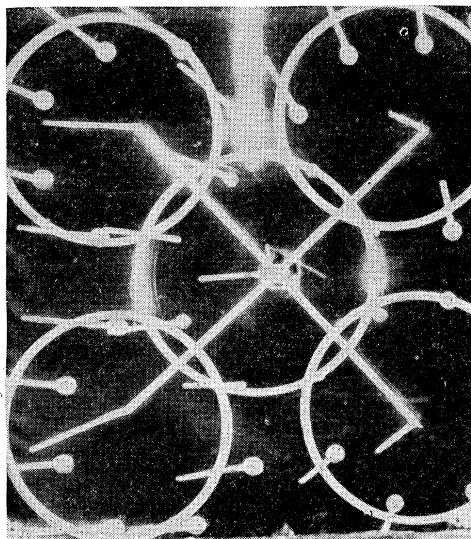


FIG. 2. A neutral particle interacts with a helium nucleus to produce two charged secondary particles in the central ionization chamber just above the anode (10 600-ft elevation).

circuit that allowed pulses greater than a given size to pass from the amplifier to the control circuit. Throughout the experiment only pulses greater than 1.5 times a polonium-alpha pulse were permitted to trigger the chamber. This minimum corresponds to an energy release of 8 Mev by ionization in the gas of the chamber.

Stereo photographs were taken at an angular separation of 12 degrees between the two optic axes.

III. EXPERIMENTAL PROCEDURE AND RESULTS

The cloud chamber was operated at sea level for 5 months and at 10 600-ft elevation (White Mountain, California) for 3 months. At the higher altitude the chamber was filled successively with argon, neon,²

¹ Lewis, Brown, SeEVERS, and HONES, *Rev. Sci. Instr.* **22**, 259 (1951).

² Thirty cubic feet of high purity neon were donated by the Linde Air Products Company for use in this part of the experiment.

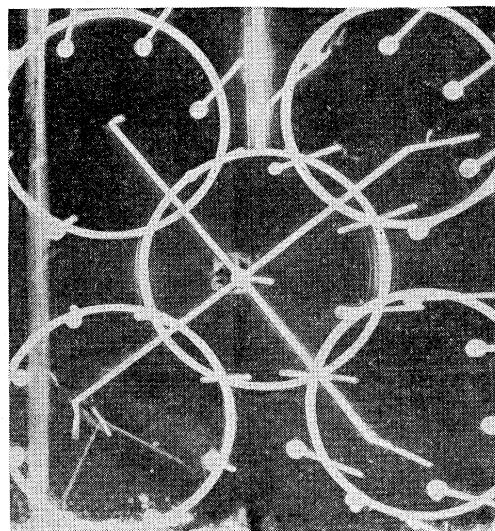


FIG. 3. An interaction of a neutral particle with a nitrogen nucleus in which four charged secondaries are produced in the lower left ionization chamber (10 600-ft elevation).

helium, and nitrogen. At sea level the operation was carried out only with an argon filling. During part of the argon run at high altitude, layers of brass absorber were placed immediately above the cloud chamber. The operating conditions throughout the experiment together with the numbers of photographs taken and numbers of nuclear interactions observed in each gas are summarized in Table I. The sensitive time in each case is the difference between the total operating time

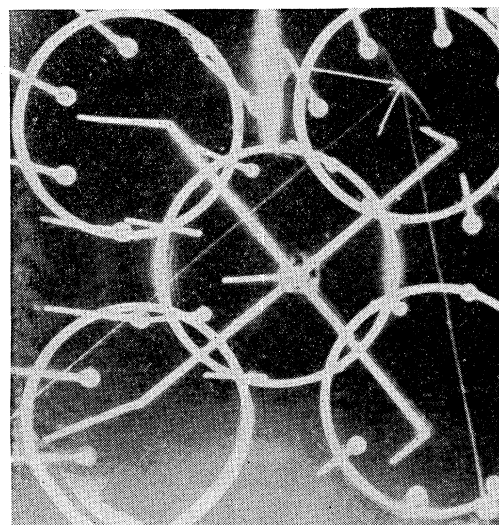


FIG. 4. Seven charged secondary particles are produced in the upper right ionization chamber by the interaction of a neutral particle with a neon nucleus. The whisp of droplets pointing toward the anode are from negative ions formed as some of the electrons heading toward the anode are captured (10 600-ft elevation).

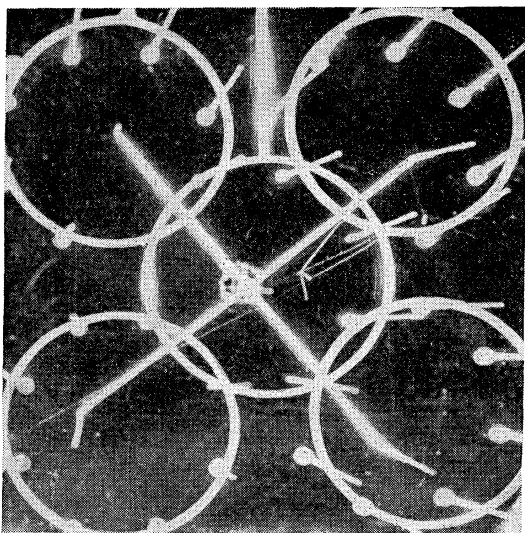


FIG. 5. In the original photograph six charged particles can be distinguished in the nuclear interaction with an argon nucleus in the upper right ionization chamber. One of the lightly ionizing particles lies in the upper hemisphere and may be the primary particle. One of the secondary particles interacts with another argon nucleus in the central ionization chamber to produce four heavily ionizing particles (10 600-ft elevation).

and the product of the chamber dead time and the number of photographs taken.

Of the total of 9210 cloud chamber expansions occurring in the experiment, 30 percent were triggered by nuclear interactions in the gas, 22 percent by nuclear interactions in solid material, 7 percent by extensive air showers, and 41 percent by spurious pulses arising

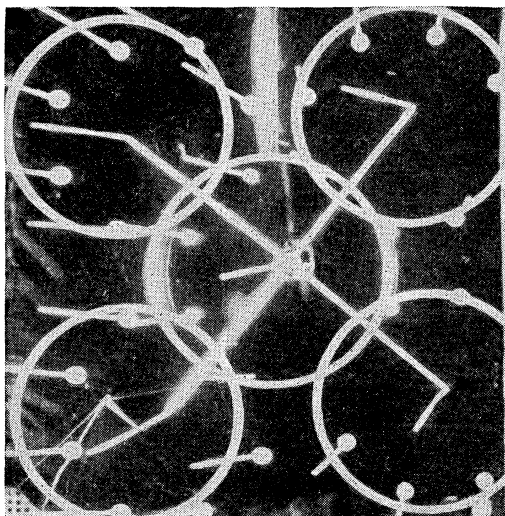


FIG. 6. In this nuclear interaction in argon in the lower left-hand chamber, 13 nearly minimum ionizing particles are involved. Three of these lie in the upper hemisphere. Of the ten moving downward, seven lie in a narrow cone. The thick whisp of droplets is from capture of some of the electrons on their way to the anode (sea level).

from lightning and other causes. Figures 2, 3, and 4 are examples of nuclear interactions occurring in the gases helium, nitrogen, and neon, respectively, and Figs. 5, 6, and 7 are examples of interactions in argon.

IV. ALTITUDE VARIATION

From the data of Table I the ratio of the rate of occurrence of nuclear interactions in argon at 10 600-ft elevation to that at sea level at the same gas pressure is 12.5 ± 1.0 . This corresponds to an absorption mean free path in air, for the total flux of N radiation, of $132 \pm 4 \text{ g cm}^{-2}$, in fair agreement with the value 138 g cm^{-2} obtained from the altitude variation of burst rates in thin-walled ionization chambers.³

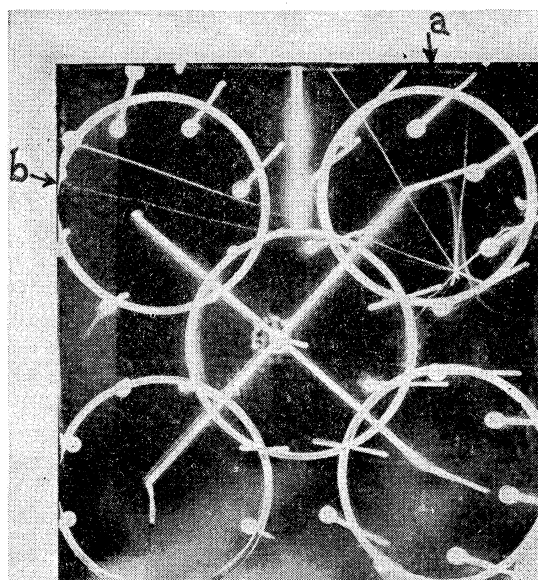


FIG. 7. A nuclear interaction in argon in which 12 charged particles are involved. Four of them are nearly minimum ionizing. Of these, particle (a) is probably the primary. The apparent deviation in the direction of particle (b) as it passes near the anode of the upper left chamber is just the result of motion of the positive ions in the intense electric field that exists near the anode before being cut off (10 600-ft elevation).

V. SIZE OF THE INTERACTIONS

The numbers of nuclear interactions occurring in each of the four gases studied are listed in Table II according to the total number of charged particles observed in each interaction irrespective of their being primary or secondary particles. All tracks longer than 2 mm were counted. No direction could be assigned to groups of ions covering dimensions smaller than this.

There is a general decrease in the size of the interactions, as far as numbers of charged particles are concerned, with the size of the target nucleus. Though lightly ionizing particles are included in the above table, this result is qualitatively in agreement with the

³ B. Rossi, *Revs. Modern Phys.* 20, 537 (1948).

conclusion, from sandwich emulsion work,⁴ that nuclear interactions (stars) generated in the oxygen and smaller nuclei of the emulsion have less than 6 heavily ionizing prongs.

VI. ANGULAR DISTRIBUTIONS OF THE PRIMARY AND SECONDARY PARTICLES

The zenith angles of the trajectories of the charged particles involved in each nuclear interaction occurring in the gas were measured as follows. The cloud chamber photographs were reprojected through an optical system identical with that of the camera onto a screen that could be set in any direction and was provided with scales such that when the two images of a given track were brought into conjunction the zenith angle of the track could be read directly to within 1 or 2 degrees. So that the accuracy of measurement would be kept within these limits, the zenith angles of only those particles having a range greater than 5 mm were measured.

Since the direction of motion of the more lightly ionizing particles, some of which may be initiating

TABLE II. Numbers of nuclear interactions observed to occur in the gases A, Ne, N, and He, classified according to the number of charged particles associated with each interaction.

Gas	Elevation, feet	Absorber above cloud chamber, in. brass	Number of charged particles										
			1	2	3	4	5	6	7	8	9	10	>10
A	10 600	0	179	214	235	159	127	75	46	25	17	14	21
A	10 600	0.25	22	32	46	27	25	12	6	2	3	2	2
A	10 600	0.75	45	94	77	69	43	14	14	8	9	2	4
A	s.l.	0	100	89	107	81	46	28	20	10	8	5	7
Ne	10 600	0	1	14	24	10	10	4	3	1			
N	10 600	0	80	99	141	96	21	2					
He	10 600	0	102	4									

particles, could not be determined, they were regarded, for the purposes of the above measurement, as emanating from the points of origin of the nuclear interactions.

In all of the observed interactions produced in the gas and involving only one charged particle of range greater than 2 mm, the particle both started and terminated in the gas. The end representing the point of origin of such an interaction could often be distinguished by the presence of a glob of ionization, probably attributable to the recoil nucleus, whereas at the terminus distinguishing features were an increase in ionization (widening of the track) or small deviations of the direction of motion of the particle.

The distribution in zenith angle of the trajectories of the charged particles involved in nuclear interactions in argon at high altitude and at sea level are shown in Fig. 8. The distributions of particles having ionization less than twice minimum (lightly ionizing particles) and those greater than twice minimum (heavily ionizing particles) have been plotted separately. The data

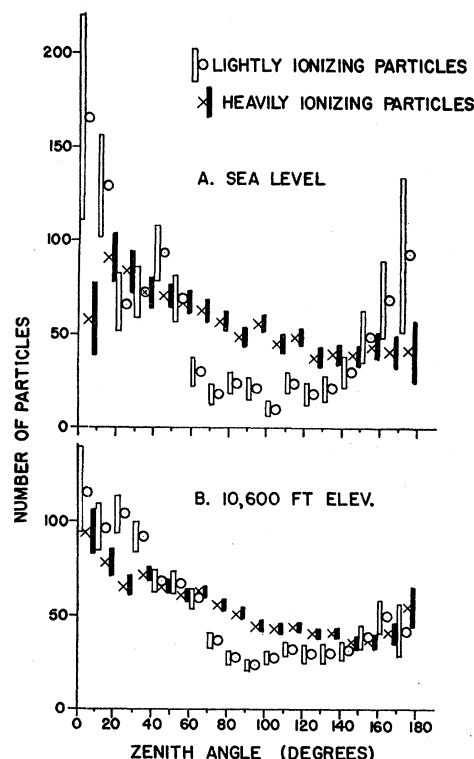


FIG. 8. Zenith-angle distributions of the lightly (<2 times minimum) and heavily (>2 times minimum) ionizing particles associated with nuclear interactions in argon at sea level and 10 600-ft elevation. Ordinates are proportional to the numbers of particles per steradian. All curves have been normalized to the same area. Zero-zenith angle corresponds to the vertically downward direction.

from all of the argon runs at high altitude have been combined. All curves have been normalized to the same area for purposes of comparison.

The heavily ionizing particles show a preference for the downward (zenith angles less than 90°) over the upward hemisphere to about the same degree at both altitudes. At both altitudes the distribution of the lightly ionizing particles can be separated into two groups, one concentrated in the upward and one in the downward direction. The former group may be interpreted as consisting, in part at least, of initiating particles belonging to the charged *N* radiation arriving from the atmosphere above the apparatus. The latter group are the high-energy protons and charged mesons that have been produced in the nuclear interactions in the argon. At sea level, where the collimating effect of the atmosphere has had more influence, the interacting charged *N* radiation arriving from the vertical is seen from Fig. 8A to be about 6 times the intensity of the horizontal, lightly ionizing particles, whereas at 10 600-ft elevation this ratio is only 2. This is in qualitative agreement with the results of photographic plate work⁵ in which the distribution of the zenith angle of star-

⁴ J. B. Harding, Nature 163, 440 (1949).

⁵ R. H. Brown et al., Phil. Mag. 40, 862 (1949).

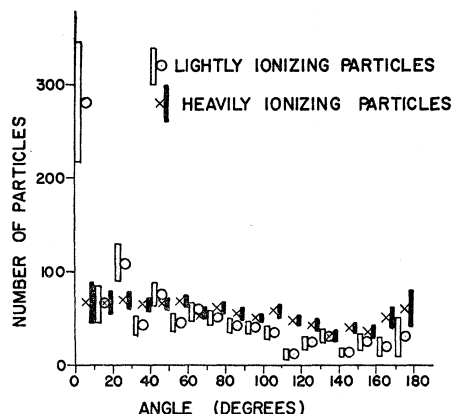


FIG. 9. Angular distributions of the heavily and lightly ionizing particles produced in argon at 10 600-ft elevation about the direction of the charged particles producing them. Ordinates are proportional to the number of particles per steradian.

particle trajectories projected onto a vertical plane were studied.

On the assumption that the lightly ionizing particles in the upper hemisphere are charged N rays, the angles between them and the directions of the secondary particles they produce were measured directly from the projected cloud chamber photographs. Whenever, in a single nuclear interaction, there were two or more lightly ionizing particles in the upper hemisphere that showed no distinguishable difference in ionization, the one nearest the vertical was selected as the N ray. The angular distributions of the heavily and lightly ionizing secondary particles are given in Fig. 9 for the interactions occurring in argon at 10 600-ft elevation. The collimation of the lightly ionizing secondaries about the direction of the particle assumed to be the initiator is further evidence favoring this assumption. The heavily ionizing secondaries show a less pronounced preference to move in the direction of the primary particle.

VII. RATIO OF THE NUMBERS OF CHARGED AND NEUTRAL N RAYS

In the argon high-altitude runs in which no absorber was above the cloud chamber, there was a total of 236 nuclear interactions in which one or more lightly ionizing particles lie in the upper hemisphere. If these are produced by charged N rays and the remaining 876 interactions, observed during the same runs, by neutral N rays, their ratio, 0.27 ± 0.02 , may be taken as a measure of the ratio of the number of charged to neutral N rays arriving at this elevation. It will be the true ratio only if the charged and neutral N rays have the same average cross section for the production of the observed nuclear interactions. The charged fraction is favored in this analysis because the neutral N rays may be expected to send some lightly ionizing secondaries in the upward direction that would be classed incorrectly as charged primary particles.

At sea level the observed ratio is 0.18 ± 0.02 . The lower value is consistent with the atmospheric absorption of the charged N component being more rapid than the neutral part because of ionization loss.

The observed ratios are those which occur in a region separated from the atmosphere by heavy walls ($\frac{1}{2}$ inch of brass or $1\frac{1}{4}$ inches of glass) and may be expected to be somewhat different from the natural ratio.

VIII. ABSORPTION OF THE N RADIATION

Before reaching the gas in the sensitive volume of the cloud chamber, the N radiation must pass through the $\frac{1}{2}$ -inch brass roof. To investigate the influence of the roof on the number of nuclear interactions observed, the cloud chamber was run with additional layers of brass above it as indicated in Fig. 1. The rates of occurrence of nuclear interactions in argon at 10 600-ft elevation calculated from the observed data listed in Table I are plotted in Fig. 10 as a function of the total absorber thickness (roof plus added brass) separating the N radiation from the contained gas. Also plotted in Fig. 10 are the observed rates subdivided into two groups, one including all interactions involving more than one charged particle and the other all interactions involving only one charged particle. If an exponential variation is assumed, extrapolation of the latter two curves to zero roof thickness gives the result that the true rates of occurrence of nuclear interactions involving only one or more than one charged particle are 1.34 ± 0.20 and 1.06 ± 0.06 times greater, respectively, than the rates observed under the normal $\frac{1}{2}$ -inch brass roof.

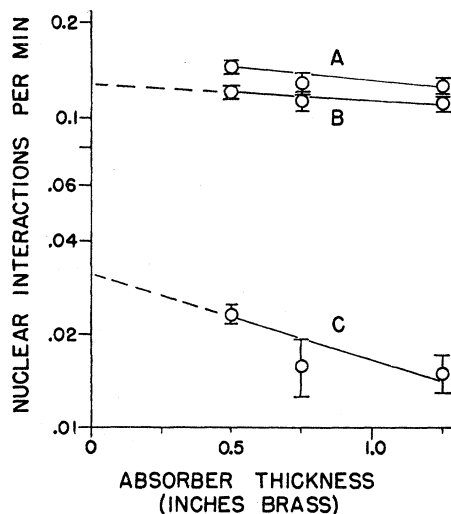


FIG. 10. Dependence of the rate of occurrence of nuclear interactions in argon at 10 600-ft elevation on the amount of absorber between the atmosphere and the interior of the cloud chamber: A, all interactions; B, interactions involving more than one charged particle; C, interactions involving only one charged particle.

IX. EFFICIENCY OF THE IONIZATION CHAMBER

By means of the projection system already described, the geometric location of the point of origin of each nuclear interaction occurring in the gas was determined. The coordinates measured were the distances of each point of origin from (i) the vertical plane containing the five end points of the ionization chamber anodes nearest the camera (see Fig. 1) and from (ii) the central anode wire of the ionization chamber within which the interaction originated.

The length of each ionization chamber was divided into ten equal intervals, and the numbers of origin coordinates, defined by (i) above, falling in each interval were counted. The full-line histogram in Fig. 11 is the distribution of the interaction origins among these intervals for all of the observed interactions occurring in the monatomic gases argon, neon, and helium at sea level and high altitude combined. This included the 2344 interactions listed in Table I plus 83 others that occurred during runs for which the sensitive time was not measured. A total of 806 interactions occurs in the front half of the ionization chamber assembly while 1621 occur in the rear half. The front half of the ionization chamber is therefore $806/1621 = 0.50 \pm 0.02$ as efficient as the rear. A similar plot for the nuclear interactions occurring in nitrogen (broken-line histogram of Fig. 11) gives the result that the front half of the ionization chamber is 0.39 ± 0.04 as efficient as the rear half when filled with this gas.

The volume of each ionization chamber was divided into 10 radial intervals coaxial with the anode wire. The radii of the cylinders defining the intervals were so chosen as to make the volumes of the intervals equal. The number of radial coordinates, defined by (ii) above, falling in each interval were counted for the nuclear

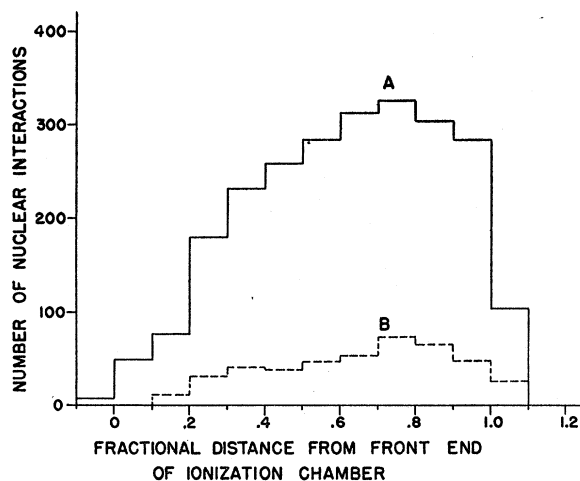


FIG. 11. The distribution of the points of origin of the nuclear interactions along the length of the ionization chamber assembly. Ordinates are numbers of interactions occurring per tenth of the chamber length. *A*, for interactions occurring in helium, neon, and argon at sea level and 10 600 ft combined; *B*, for interactions occurring in nitrogen at 10 600-ft elevation.

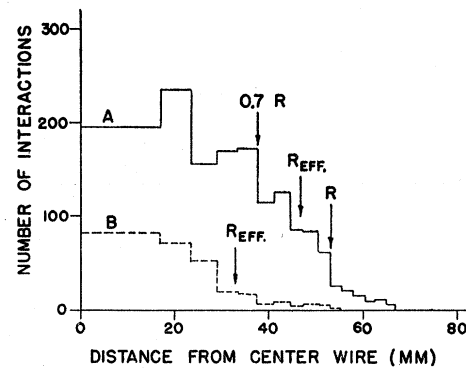


FIG. 12. Distribution of the distances of the points of origin of the nuclear interactions from the central wire of the ionization chamber in which they occurred. The radial intervals along the horizontal axis correspond to equal volume intervals in the ionization chamber. *A*, for interactions occurring in helium, neon, and argon at sea level and 10 600 ft combined; *B*, for interactions occurring in nitrogen at 10 600-ft elevation. *R* is the geometric radius of an ionization chamber. The ordinates are numbers of interactions per radial interval.

interactions in argon, neon, and helium, occurring in the more sensitive region (0.5 to 1.0 of the geometric length) of each ionization chamber. The distribution of the points of origin in the radial intervals is given by the full-line histogram of Fig. 12 for all five ionization chambers combined. Out to 0.71 of the geometric radius, *R*, the distribution is nearly uniform as would be expected if the ionization chambers were highly efficient in this region. Beyond this radius the distribution gradually drops to zero. An effective radius may be defined as $0.71R + r$, where r is the area under the histogram beyond $0.71R$ and f is the average frequency of occurrence of nuclear interactions per radial interval from zero to $0.71R$. The efficiency of the rear part of the ionization chamber, defined as the detected fraction of the nuclear interactions occurring within its geometric boundaries, is $[(0.71R + r)/R]^2$. From Fig. 12 a value of $[(47.1 \pm 0.5)/53]^2 = 0.79 \pm 0.02$ is obtained. The efficiency of the complete ionization chamber assembly is thus $0.79(0.50 + 1)/2 = 0.59 \pm 0.014$ when filled with a monatomic gas.

The broken-line histogram of Fig. 12 is the radial distribution of points of origin of the nuclear interactions in nitrogen. Calculations similar to those above give 33.0 ± 0.6 mm as the effective radius and 0.27 ± 0.01 as the over-all efficiency of the ionization chamber when filled with this gas. The lower efficiency is caused by the higher percentage of electron capturing impurities in the nitrogen used.

X. NATURAL RATE OF OCCURRENCE OF COSMIC-RAY NUCLEAR INTERACTIONS

The observed rates of occurrence of nuclear interactions in the four gases at 10 600-ft elevation calculated from the data of Table I for which there was no absorber above the cloud chamber are given in the first row of Table III. The rates have been multiplied by

TABLE III. The natural rates of occurrence of cosmic-ray nuclear interactions at 10 600-ft elevation in A, Ne, N, and He. In the second row are given the rates after correcting for the inefficiency of the ionization chamber, and, in the third row after further correcting for absorption of the N component in the cloud chamber roof.

	Argon	Neon	Nitrogen	Helium
Interactions per gram atom per hour:				
Observed	4.75 ± 0.14	4.1 ± 0.5	1.34 ± 0.06	0.60 ± 0.06
Corrected for inefficiency	8.0 ± 0.3	7.0 ± 0.9	5.0 ± 0.3	1.02 ± 0.10
Corrected for roof absorption	8.9 ± 0.6	7.4 ± 1.0	5.5 ± 0.5	1.4 ± 0.3

appropriate factors so that they apply to the same number of atoms (one gram atom) of each gas. In this calculation the rates are assumed to be proportional to the quotient of the absolute pressure and temperature. The geometric volume of the ionization chamber assembly used is 9.1 ± 0.2 liters. In the second row the rates have been corrected for the inefficiency of the ionization chamber (see Sec. 9). In the third row a further correction has been applied for losses in the cloud chamber roof (see Sec. 8). In this last correction the fractions of the interactions involving one and more than one charged particle (see Table II) have been increased by factors of 1.34 ± 0.20 and 1.06 ± 0.06 , respectively.

The corrected rates of occurrence of nuclear interactions are plotted in Fig. 8 as a function of the two-thirds power of the mass number, A . The correction for losses in the cloud chamber roof is questionable because it was investigated only for the one gas, argon, it involves a considerable extrapolation, and it neglects the existence of any transition effect in the roof. The rates have been plotted both with and without this correction. Irrespective of its application, however, the general conclusion is that the rate of occurrence of cosmic-ray nuclear interactions shows no great departure from being proportional to $A^{2/3}$. The relative cross sections that the atoms present for nuclear interaction to the cosmic-ray N component are therefore nearly the same as their relative geometric nuclear cross sections.

For an incoming integrated flux of N radiation of 6.0×10^{-3} particle $\text{cm}^{-2} \text{sec}^{-1}$, the expected rate of occurrence of nuclear interactions per gram atom of an element would be that given by the straight line in Fig. 13 if the cross section for interaction were truly geometric. This flux is somewhat higher than estimates

of the N -component flux that can be made from measurements of the number of stars $\text{cm}^{-3} \text{day}^{-1}$ occurring in nuclear emulsions.^{6,7} The higher value is to be expected since the interactions involving one and two charged particles that are omitted in emulsion studies are counted in the present work. The true flux may be still higher than the above value since interactions in which less than 8 Mev of the energy released to charged particles is dissipated within the ionization chamber are not counted. This omitted group would be made up partly of interactions of some of the low-energy neutrons and protons and partly of interactions of high-energy neutrons and protons in which only

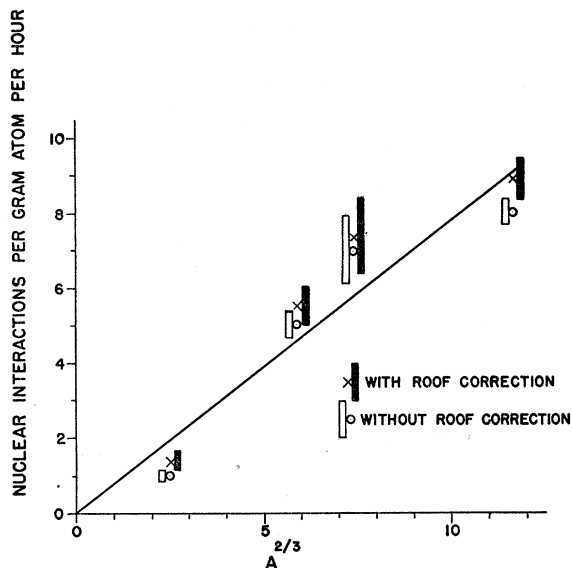


FIG. 13. The rate of occurrence of cosmic-ray nuclear interactions at 10 600 ft per gram atom of an element as a function of the two-thirds power of the mass number of the element. The straight line is the rate expected for a total flux of N radiation of $6.0 \times 10^{-3} \text{ cm}^{-2} \text{ sec}^{-1}$ if the cross section for interaction is geometric.

lightly ionizing or neutral secondary particles were produced.

The author wishes to thank Professor W. M. Nielson for his interest in this work. Much of the work of analyzing the photographs was done by Mrs. Jane Brown.

⁶ Bernardini, Cortini, and Manfredini, Phys. Rev. **79**, 952 (1950).

⁷ J. J. Lord, Phys. Rev. **81**, 901 (1951).

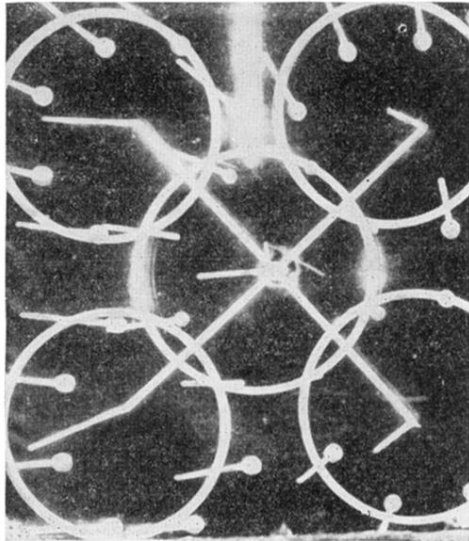


FIG. 2. A neutral particle interacts with a helium nucleus to produce two charged secondary particles in the central ionization chamber just above the anode (10 600-ft elevation).

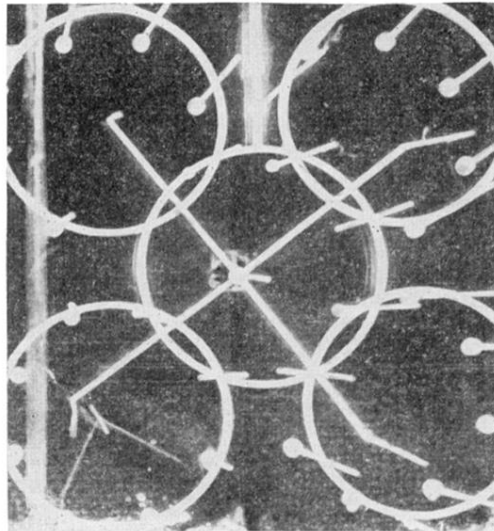


FIG. 3. An interaction of a neutral particle with a nitrogen nucleus in which four charged secondaries are produced in the lower left ionization chamber (10 600-ft elevation).

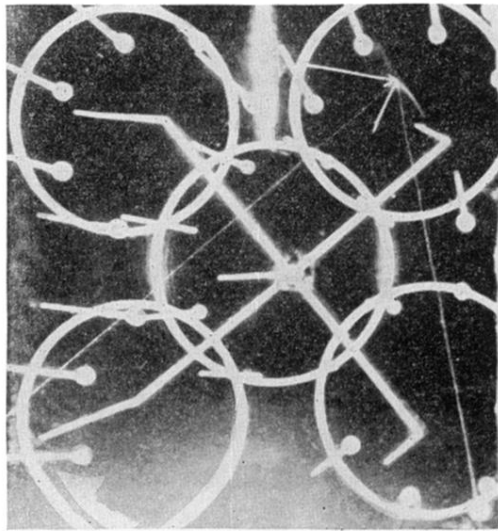


FIG. 4. Seven charged secondary particles are produced in the upper right ionization chamber by the interaction of a neutral particle with a neon nucleus. The whisp of droplets pointing toward the anode are from negative ions formed as some of the electrons heading toward the anode are captured (10 600-ft elevation).

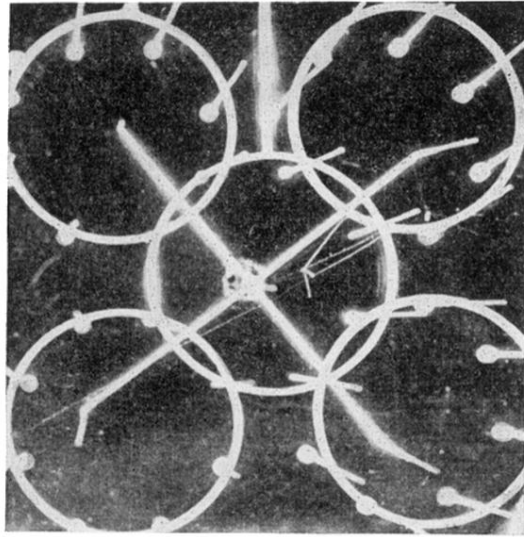


FIG. 5. In the original photograph six charged particles can be distinguished in the nuclear interaction with an argon nucleus in the upper right ionization chamber. One of the lightly ionizing particles lies in the upper hemisphere and may be the primary particle. One of the secondary particles interacts with another argon nucleus in the central ionization chamber to produce four heavily ionizing particles (10 600-ft elevation).

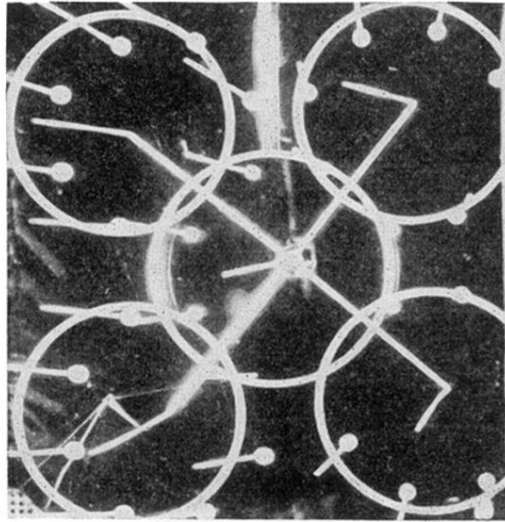


FIG. 6. In this nuclear interaction in argon in the lower left-hand chamber, 13 nearly minimum ionizing particles are involved. Three of these lie in the upper hemisphere. Of the ten moving downward, seven lie in a narrow cone. The thick whisp of droplets is from capture of some of the electrons on their way to the anode (sea level).

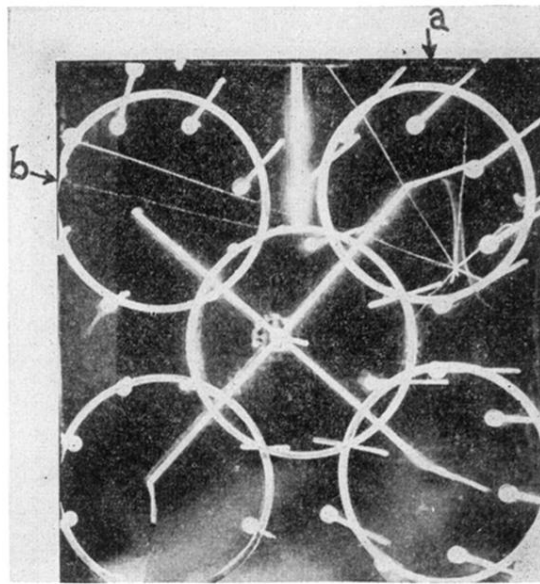


FIG. 7. A nuclear interaction in argon in which 12 charged particles are involved. Four of them are nearly minimum ionizing. Of these, particle (a) is probably the primary. The apparent deviation in the direction of particle (b) as it passes near the anode of the upper left chamber is just the result of motion of the positive ions in the intense electric field that exists near the anode before being cut off (10 600-ft elevation).